

Optimized δ - Expansion for Lattice U(1) and SU(2) with Interpolating Continuum Action

Iring Bender and Dieter Gromes

Institut für Theoretische Physik der Universität Heidelberg
Philosophenweg 16, D-69120 Heidelberg
E - mail: i.bender@thphys.uni-heidelberg.de
d.gromes@thphys.uni-heidelberg.de

Abstract: Embedding the lattice gauge theory into a continuum theory allows to use the continuum action as trial action in the variational calculation. Only originally divergent graphs contribute. This leads to a very simple scheme which makes it possible to write down explicit expressions for the plaquette energy E for U(1) in arbitrary space time dimension for the first three orders of the expansion. For dimensions three and four one can even go up to fourth order. This allows a rather thorough empirical investigation of the convergence properties of the δ -expansion, in particular near the phase transition or the transition region, respectively. As already found in previous work, the principle of minimal sensitivity can be only applied for β above a certain value, because otherwise no extremum with respect to the variational parameter exists. One can, however, extend the range of applicability down to small β , by calculating instead of E some power E^κ , or by performing an appropriate Padé transformation. We find excellent agreement with the data for β above the transition region for the second and higher orders. Below the transition region the agreement is rather poor in low orders, but quite impressive in fourth order. For SU(2) we performed the calculation up to second order. The agreement with the data is somewhat worse than in the abelian case.

April 1996

1 Introduction

The “optimized δ - expansion”, also called “linear δ - expansion”, or, more appropriately, “variational perturbation theory”, is a powerful method which combines the merits of perturbation theory with those of variational approaches. The underlying idea is simple: The action S is split into a free part λS_0 and an interacting part $S - \lambda S_0$. Actually it is not necessary that S_0 describes a free action, but only that all relevant quantities can be calculated explicitly with S_0 . The interacting part is multiplied by a factor δ which serves as expansion parameter and is put equal to one at the end. The exact result should be independent of the parameter λ while any approximation will depend on it. The idea, often called “Stevenson’s principle of minimal sensitivity” [1], is that the approximate solution should depend as little as possible upon the parameter λ . This means that λ should be chosen such that the quantity to be calculated has an extremum. In this way the result becomes non-perturbative because λ becomes a non-linear function of the coupling constant. In every order of perturbation theory the parameter has to be calculated again. There are already many successful applications of this method in various fields of physics as well as rigorous convergence proofs for simple cases. We refer, e.g. to the references given in [2]. In the present paper we concentrate on applications on the lattice. Up to now, three different types of actions S_0 have been used in this context.

In the first paper on the subject by Duncan and Moshe [3], which, among other topics, treats the plaquette energy for $U(1)$ and Z_2 gauge theory in $d = 3$ space time dimensions, the action S_0 was chosen as a maximal tree of plaquettes. This is a set of plaquettes which does not contain a closed surface, whereas the addition of any further plaquette would lead to a closed surface. One of the reasons for this choice is, of course, that all integrations can be performed explicitly in this case. A maximal tree for S_0 was also used by Buckley and Jones [6] in their work on $Z(2)$, $U(1)$, and $SU(2)$ in four dimensions.

A second natural choice for S_0 is a quadratic action, typically the sum of the squares of the plaquette angles. Such an action was used by Duncan and Jones [4] in their work on $U(1)$ in $d = 4$ and by Buckley and Jones [5] for $SU(2)$.

A third choice, used by Akeyo and Jones [7] for $SU(2)$, as well as for the mixed $SU(2)$ - $SO(3)$ model, is a single link action, i.e. the sum of $\text{Tr } U_l$ over all links.

A maximal tree is a good approximation to the original action in the strong coupling limit. A quadratic action or a single link action, on the other hand, is a good approximation in the weak coupling limit. The δ - expansion therefore behaves quite differently in the two cases: In the first case one obtains a good description of the Monte Carlo data for small β , roughly up to the phase transition, or the transition region, respectively. In the second case the same holds for large β from the transition region up to infinity.

The signal for the qualitative change in the behavior is the merging of two extrema (with respect to λ) into a point of inflexion with horizontal tangent and its subsequent disappearance, when β is changed near the critical region. We will, however, see, that this point of inflexion has no special relevance.

In the present paper we use a fourth ansatz for S_0 which has several advantages compared to the previous ones (as well as a minor drawback). We enlarge the degrees of

freedom of the system by embedding the lattice gauge theory into a continuum theory and use the free Maxwell Lagrangian for the vector potential as our interpolating action. The divergences which arise in the continuum are absorbed by splitting off a divergent factor from the action. The consequence thereof is that only originally divergent graphs, in which a photon line starts and ends at one and the same link, survive. This leads to a dramatic simplification. No graph has to be calculated explicitly, the whole game essentially becomes a problem of counting certain configurations of plaquettes. The advantages of the method are the following:

- In any order of the calculation we obtain neither integrals, nor infinite sums, nor special functions.
- In any order n of the expansion only a finite number of configurations, consisting of $n + 1$ connected plaquettes, has to be considered.
- In any order the result only contains polynomials in the variational parameter λ and powers of $e^{-\lambda/4}$.
- The calculation can be easily performed for arbitrary dimension.

These features allow calculations to a comparatively high order. In the present paper we obtained explicit expressions for arbitrary dimension $d \geq 3$ up to third order of the δ - expansion. For the cases $d = 3$ and $d = 4$, with the help of a computer program which searches the relevant configurations of plaquettes, we can go to fourth order, one order more than computed in [4].

We also mention here a drawback of the method:

- The coefficient in front of $1/\beta$ in the weak coupling expansion is not correctly reproduced from the beginning, but it converges to the correct value in higher orders.

Since our main interest is in the transition region, this drawback can be easily tolerated. A priori it is anyhow impossible to tell which type of trial action is best suited in this region.

In sect. 2 we explain our method for U(1) and give the relevant general formulae. In sect. 3 we present the results up to order 4. Here we also discuss possibilities to enlarge the region in β where the principle of minimal sensitivity can be applied. In sect. 4 we extend the method to SU(2) and apply it up to second order. Sect. 5 summarizes our conclusions.

2 The method for U(1)

We use the familiar formulation of U(1) on a d -dimensional lattice with lattice constant a , described by the partition function

$$Z = \int_{-\pi}^{\pi} \cdots \int_{-\pi}^{\pi} e^{-\beta S} \prod_l \frac{d\phi_l}{2\pi}, \quad (2.1)$$

with the action

$$S = - \sum_{p'} \cos \Theta_{p'}. \quad (2.2)$$

Here l runs over the links, p' over the plaquettes, $\Theta_{p'}$ is the sum of the four (oriented) angles ϕ_l living on the links of the plaquette p' . The object we shall discuss is the average plaquette energy E , i.e. the expectation value of $\cos \Theta_p$.

In the first step we want to extend the integrations over the angles ϕ_l to the interval from $-\infty$ to ∞ . This can be done by using the following relation which holds for any periodic function $f(\phi)$:

$$\int_{-\pi}^{\pi} f(\phi) \frac{d\phi}{2\pi} = \lim_{\gamma \rightarrow 0} \sqrt{2\gamma} \int_{-\infty}^{\infty} e^{-\gamma\phi^2} f(\phi) \frac{d\phi}{2\pi}. \quad (2.3)$$

This is easily proven by splitting the rhs into integrals of length 2π , shifting the integration variable back into the interval from $-\pi$ to π , and replacing the sum over the intervals by an integral in the limit $\gamma \rightarrow 0$. Actually we will see later that in any finite order of our expansion we can simply put $\gamma = 0$ in the expectation value, which is a pleasant simplification.

In the next step we enlarge the number of degrees of freedom drastically, by introducing a vector potential A_μ defined in the whole continuum. The connection with the link variables ϕ_l is, as usual,

$$\phi_l = e \int_l A_\mu dx_\mu, \quad (2.4)$$

with $e^2 = 1/\beta$. Expectation values are not changed if we now replace the ordinary integrations $\prod_l d\phi_l/(2\pi)$ by the path integral $\mathcal{D}[A]$. The reason for this is easily understood: The fields which are not sitting on the links appear neither in the action nor in the plaquette energy. Therefore the corresponding integrations factorize both in the numerator and in the denominator and cancel. The same happens for the fields which sit on the links but are transversal to them. Finally, for the longitudinal fields on the links, one may go over to new variables by performing a linear transformation with constant coefficients in such a way that one of the variables becomes the integral ϕ_l in (2.4). The integrations over the remaining other variables, as well as the constant Jacobian, cancel again and we are left with the original expectation value.

We can thus write the expectation value of the plaquette energy as an expectation value in the continuum theory:

$$E = \lim_{\gamma \rightarrow 0} \frac{1}{N_\gamma} \int E_p \exp[\beta \sum_{p'} E_{p'}] \exp[-\gamma e^2 \sum_l (\int_l A_\mu dx_\mu)^2] \mathcal{D}A, \quad (2.5)$$

with

$$E_p = \cos e \oint_p A_\mu dx_\mu. \quad (2.6)$$

The normalization constant N_γ is, of course, obtained by replacing E_p by 1 in the numerator of (2.5).

We are now in the position to apply the optimized δ -expansion by introducing the free continuum Lagrangian. All expressions in (2.5) are gauge invariant in the limit $\gamma \rightarrow 0$, so, for simplicity, we will use the Feynman gauge which has the advantage that all graphs connecting orthogonal links vanish from the beginning. While, on the lattice, everything is finite, we will immediately obtain divergences in the continuum from the singularity of the propagator at zero distance. At first sight this looks like an additional complication. It can, however, easily be overcome by splitting off an appropriate divergent constant from the free action. In fact, this leads to a drastic simplification, because only the divergent terms of ordinary perturbation theory survive. This, in turn, will have the consequence that in any order only finite connected sets of plaquettes are involved.

As free interpolating action we choose

$$S_0 = -\frac{c}{\beta\lambda} \int A_\mu \square A_\mu d^d x. \quad (2.7)$$

Here λ is the variational parameter. The constant c is a positive parameter which is divergent for $d \geq 3$. It is formally defined by

$$c = -\int_0^a \int_0^a D(t-t') dt dt' \quad (2.8)$$

with D the Green function of the d'Alembert operator, e.g. in four dimensions $D(x) = -1/(4\pi^2 x^2)$. Of course, one could easily use some regularization which would lead to a large but finite c , and later on perform the limit. Because the whole procedure is, however, very transparent, this intermediate step can be skipped.

After introducing the free continuum action, the plaquette expectation value in the optimized δ -expansion reads

$$E = \frac{1}{N(\delta)} \int E_p e^{-S_0} e^{\delta(S_0 + \beta \sum_{p'} E_{p'})} \mathcal{D}A. \quad (2.9)$$

We have simplified the expression by taking the limit $\gamma \rightarrow 0$ in (2.5) which is now allowed in any finite order of the δ -expansion.

The problem has thus become a continuum problem of calculating expectation values of products of plaquettes. The calculations for higher orders are greatly simplified by a simple trick, essentially already used in [3]. One should *not* expand the expression (2.9) with respect to δ as it stands, because this would introduce all the mixing terms between S and S_0 . Things become much simpler if one leaves the term $(1-\delta)S_0$ together and performs the substitution

$$A_\mu = \sqrt{\frac{\beta\lambda}{2c(1-\delta)}} A'_\mu. \quad (2.10)$$

This brings the free action into the usual form $(1-\delta)S_0 \rightarrow S'_0 = -(1/2) \int A'_\mu \square A'_\mu d^d x$. In E_p and $E_{p'}$ as defined in (2.6) one has to make the replacement

$$e \rightarrow e' = \sqrt{\frac{\tilde{\lambda}}{2c}}, \quad (2.11)$$

where, for convenience, we have introduced the abbreviation

$$\tilde{\lambda} \equiv \lambda/(1 - \delta). \quad (2.12)$$

The quantity β stays as it was before. So we end up with the comparatively simple expression

$$E = \int E_p e^{-S'_0} e^{\delta\beta \sum_{p'} E_{p'}} \mathcal{D}A' / \int e^{-S'_0} e^{\delta\beta \sum_{p'} E_{p'}} \mathcal{D}A' \quad (2.13)$$

in which now e and A_μ are to be replaced by e' and A'_μ in E_p and $E_{p'}$. Note, that besides the explicit δ -dependence of this expression, there is also an implicit δ -dependence contained in e' which has to be considered.

Let us first look for the expectation value of the 1×1 Wilson loop with respect to the free continuum action. There are two types of graphs: In the first type the propagator connects two different parallel lines of the loop and is finite. The coupling constant e'^2 multiplying the propagator vanishes due to the constant $c = +\infty$ in the denominator. Therefore the product is zero, i.e. the exponential becomes equal to 1. We therefore only get contributions from the self energy graphs where the propagator connects points on the same link. For the four links of the plaquette this gives

$$\exp\left\{\frac{4}{2}e'^2 \int_0^a \int_0^a D(t-t') dt dt'\right\} = \exp(-\tilde{\lambda}) = \exp(-\lambda/(1-\delta)). \quad (2.14)$$

Our choice for the divergent constant c in (2.8) becomes clear from this. In any order of the δ -expansion the β^0 term is immediately obtained by expanding (2.14) to the desired order in δ .

To obtain the complete result we have to expand (2.13). After symmetrization in the summation variables p_k one obtains a series of the form

$$E^{(n)} = \sum_{\nu=0}^n \frac{\eta_\nu^{[n]}}{\nu!} \delta^\nu \beta^\nu \quad (2.15)$$

with

$$\begin{aligned} \eta_0 &= \langle E_p \rangle \\ \eta_1 &= \sum_{p_1} [\langle E_p E_{p_1} \rangle - \langle E_p \rangle \langle E_{p_1} \rangle] \\ \eta_2 &= \sum_{p_1, p_2} [\langle E_p E_{p_1} E_{p_2} \rangle - \langle E_p \rangle \langle E_{p_1} E_{p_2} \rangle - \langle E_{p_1} \rangle \langle E_p E_{p_2} \rangle \\ &\quad - \langle E_{p_2} \rangle \langle E_p E_{p_1} \rangle + 2 \langle E_p \rangle \langle E_{p_1} \rangle \langle E_{p_2} \rangle] \\ \dots &= \dots\dots\dots \\ \eta_n &= \sum_{p_1, \dots, p_n} [\langle E_p E_{p_1} \dots E_{p_n} \rangle - \text{factorized contributions}]. \end{aligned} \quad (2.16)$$

Here $\langle \dots \rangle$ denotes the normalized expectation value. The coefficients $\eta_\nu^{[n]}$ in (2.15) are defined by expanding each $\eta_\nu(\tilde{\lambda})$ with respect to the δ contained in $\tilde{\lambda}$ up to order $n - \nu$. This means that in total one expands up to order n of the δ -expansion. Finally one has to put $\delta = 1$.

The calculation of the expectation values proceeds along the following scheme. Consider, e.g. the term $\langle E_p E_{p_1} \dots E_{p_n} \rangle$. Write the cosines in the E_{p_k} as exponentials, $\cos \Theta_k = (1/2) \sum_{j_k = \pm 1} e^{ij_k \Theta_k}$, the cosine in E_p can be simply replaced by $e^{i\Theta}$. In this way one obtains a sum of 2^n terms with a factor 2^{-n} in front. The expectation value above is then evaluated with the use of the formula

$$\frac{\int e^{-S'_0} e^{\int J'_\mu(x) A'_\mu(x) d^d x} \mathcal{D}A'}{\int e^{-S'_0} \mathcal{D}A'} = \exp\left\{-\frac{1}{2} \int J'_\mu(x) D(x-x') J'_\mu(x') d^d x d^d x'\right\}. \quad (2.17)$$

In our case all currents J'_μ are localized on the links and the d -dimensional integrals above become one dimensional. The current on a link has the form

$$J_{link} = ie' \delta^{(d-1)}(link) \sum_k j_k^{(link)}, \quad (2.18)$$

where $\delta^{(d-1)}(link)$ is the $(d-1)$ -dimensional δ -function with support on the link while the sum runs over all plaquettes p_k which share the considered link (put $p = p_0, j_0 = 1$ in this context). The further calculation is greatly simplified by the fact that we never need any mixing terms between different links, because these involve a finite propagator, so the exponent becomes zero due to the factor c in the denominator of e'^2 . For the singular diagonal contribution of a single link, on the other hand, the divergent constant c cancels and we end up with $-(\sum_k j_k^{(link)})^2 \tilde{\lambda}/4$ in the exponent. Finally, we thus obtain the generic formula

$$\langle E_p E_{p_1} \dots E_{p_n} \rangle = \frac{1}{2^n} \sum_{j_{k_1}, \dots, j_{k_n} = \pm 1} \exp\left\{-\sum_{links} \left(\sum_k j_k^{(link)}\right)^2 \tilde{\lambda}/4\right\}. \quad (2.19)$$

This allows all expressions in (2.16) to be evaluated in a simple way.

An enormous simplification arises through the fact that only connected configurations of plaquettes need to be considered, where two plaquettes are called connected if they share a common link (or are identical). The reason is simple. If we have a configuration of two sets of plaquettes which are disconnected from each other, there are, as shown above, no contributions where the propagator connects the two sets. The contributions thus factorize and are therefore canceled by the factorized terms in (2.16). Therefore the expansion is local in the sense that in any order n there is only a finite number of plaquettes, coming from the expansion of the exponent of the lattice action, which needs to be considered. These plaquettes make up a connected set together with the plaquette p . Therefore we simply obtain a sum of expressions which only contain polynomials in λ (from the expansion of $\tilde{\lambda}$) times powers of $\exp(-\lambda/4)$. So, in any order we neither get integrations, nor infinite sums, nor special functions! This simple structure allows the calculation of comparatively high orders which would, e.g., become prohibitively complicated in any approach working with lattice propagators.

3 Results for U(1)

For the first three orders the plaquette configurations which contribute in the sum and their contributions can be written down explicitly. Only some modest computer help was used just for convenience. In the following we will give the formulae for general dimension d but first discuss only $d = 4$. Other dimensions are briefly treated at the end.

Order 1 and generalities

There are only two types of configurations in the sum over p_1 which contribute (see fig. 1a). In the first type one has $p_1 = p$, its contribution to η_1 , according to the foregoing considerations, is $\langle E_p^2 \rangle - \langle E_p \rangle^2 = (1/2)(1 + e^{-4\lambda} - 2e^{-2\lambda})$. The second type consists of all plaquettes p_1 which share just one link with p . Their number is $4(2d - 3)$, where the factor 4 is, of course, due to the four links of p , while the second factor counts the possible orientations of p_1 . All these plaquettes give the same contribution $\langle E_p E_{p_1} \rangle - \langle E_p \rangle \langle E_{p_1} \rangle = (1/2)(e^{-3\lambda/2} + e^{-5\lambda/2} - 2e^{-2\lambda})$. In this way one ends up with the following result.

$$E^{(1)}(\beta, \lambda) = \eta_0^{[1]} + \delta\beta\eta_1^{[1]} = (1 - \delta\lambda)e^{-\lambda} + \delta\beta\eta_1(\lambda) \quad \text{with} \quad (3.1. a)$$

$$\eta_1(\lambda) = \frac{1}{2}[1 + e^{-4\lambda} - 2e^{-2\lambda} + 4(2d - 3)(e^{-3\lambda/2} + e^{-5\lambda/2} - 2e^{-2\lambda})]. \quad (3.1. b)$$

At the end, δ has, of course, to be set equal to 1. According to the principle of minimal sensitivity we have to look for the extrema with respect to λ . There is always a local maximum at $\lambda = \infty$, corresponding to the limit, where we do not introduce an interpolating continuum action at all, i.e. to the ordinary strong coupling expansion. Choosing this extremum would obviously lead to the expected result $E^{(1)} = \beta/2$. For large β , on the other hand, there is always a minimum at small λ . This is found by expanding $E^{(1)}(\beta, \lambda) = 1 - 2\lambda + (3/2)\lambda^2 + \beta(d + 1/2)\lambda^2 + O(\lambda^3)$. The minimum is at $\lambda = 1/(d + 1/2)\beta + O(1/\beta^2)$ and gives $E^{(1)} = 1 - 1/(d + 1/2)\beta + O(1/\beta^2)$. Obviously the qualitative behavior in the weak coupling limit is correct, but the factor $1/d$ in front of β is replaced by $1/(d + 1/2)$ which means that it is too small by 11 % compared to the correct factor. The reason is, that our continuum action is not an as appropriate approximation in the weak coupling limit as, e.g. the quadratic action used in [4], [5]. We will see how this factor converges towards the correct one in higher orders. Since our main interest is in the region of the phase transition, the fact that we do not reproduce the correct weak coupling limit in first order is only a minor drawback. In this context one should also mention the merit of the variational method that it anticipates to a large extend the higher order coefficients. In our case, although it gives - 2/9 for the leading coefficient instead of - 1/4, as just discussed, it gives, e.g. a second order coefficient of -2/81 for $d = 4$. This is 79% of the correct second order term $-1/32$.

The full structure of the extrema of (3.1) is easily discussed and essentially independent of the dimension d . For large β there are 3 finite extrema (in addition to the one

at infinity), the one with the smallest λ is the minimum just discussed and has to be chosen. If β is decreased, this minimum and the neighboring maximum merge into a turning point with horizontal tangent, i.e. a point of inflexion. In the sense of catastrophe theory one has a fold catastrophe there. The value where this happens is easily found by solving the simultaneous equations $\partial E/\partial\lambda = \partial^2 E/\partial\lambda^2 = 0$. The solution is $\beta_{pi} = 0.9674$. In fig. 2a we show our results for order 1 to 4 together with the Monte Carlo data of Caldi [8]. We followed the minimum with the smallest λ when coming from large β up to the point of inflexion at β_{pi} where it disappears.

The appearance or disappearance of extrema might be interpreted as a signal for the existence of a phase transition. In fact, the value of β_{pi} found in this first order calculation is too small only by 4% compared to the value $\beta_c = 1.0081 \pm 0.0067$ given in [8]. But, on the other hand, one also finds a turning point for $d = 3$ where there is no phase transition.

There is a simple argument which shows that the point of inflexion has no direct relation to the position of the phase transition. If this were the case one should essentially obtain the same point of inflexion if, instead of E , one calculates some function of E , say a power E^κ . In the spirit of the δ -expansions one has to calculate E^κ from (3.1), expand to first order in δ , and finally put $\delta = 1$. One finds that the position of the point of inflexion depends drastically on κ . For $\kappa = 5$, e.g. one gets $\beta_{pi} = 1.6089$. If κ is decreased, β_{pi} decreases monotonically. At $\kappa_0 = 0.2781$ one reaches $\beta_{pi} = 0.8252$, while for even smaller κ there is no point of inflexion at all, while the extrema persist! If one chooses some $\kappa \leq \kappa_0$ one can therefore follow the minimum down to small β and calculate E^κ . From this one may finally obtain E .

Before we investigate, whether one can obtain reasonable results by this simple trick even below the transition region, let us first mention, that the above considerations can serve as an excellent test for the stability of the approach. Notwithstanding the fact that the point of inflexion moves with the power κ , the value of E finally obtained, should be essentially independent of κ within a reasonable range. This is indeed the case to an impressive accuracy. For illustration we choose the arbitrary value $\beta = 1.2$ and vary κ in the range from $\kappa = -1$ to $\kappa \approx 2.3$ where β_{pi} becomes equal to 1.2. The value for E then only moves from 0.7903 to 0.7868! The test becomes a bit worse if we apply it to values of β below β_{pi} , say $\beta = 0.9$, which can only be reached by the above trick for κ small enough. Varying κ from -1 to 0.6, one finds that E moves from 0.7008 to 0.6917. These values still lie considerably above the MC data but convergence to the correct values in higher orders can be expected.

One may also perform a Padé transformation with respect to δ before applying the principle of minimal sensitivity. This was done by Duncan and Moshe [3] for the second order, in order to obtain an extremum. In the first order discussed at the moment, the (0,1) Padé approximation has the interesting property that there is no turning point where the extrema disappear. Therefore one can follow the minimum over the whole range of β . This again shows that the point of inflexion has no direct relevance. It demonstrates, however, once more the impressive stability of the method for the values of β above the transition region. As seen in fig. 2b, for small β the power curve lies below the Padé curve and closer to the data, for $\beta > 1$ both curves as well as the original first order curve differ by less than 0.003.

Order 2

In second order there are 5 types of connected plaquette configurations which contribute (fig. 1b). The first two of them are identical with the ones of the first order, with one plaquette occupied twice. To count the number of equivalent configurations belonging to every type, one has to note that one of the plaquettes is always identical to the fixed plaquette p , the other two have to be arranged in all possible ways.

The discussion proceeds along the same lines as before. Contrary to the first order there is now *no* relevant minimum near $\lambda = 0$ in the weak coupling limit, so that the principle of minimal sensitivity cannot be directly applied. This is a well known feature in simple models as the anharmonic oscillator in zero and one dimension [9], where all even orders show the same behavior. In our case, there is, however, a relevant minimum for values of β around $\beta \approx 1$, which merges with a maximum at $\beta_{pi} = 1.0168$. To this belongs the value $E_{pi} = 0.6783$ in good agreement with the MC data. If one follows the minimum from the point of inflexion to increasing β one finds, however, that the curve no longer follows the data. There is no extremum which corresponds to the physical value. This is, of course, nothing but the afore mentioned absence of a reasonable weak coupling result in even orders.

To extract more useful information from the second order calculation we apply the (1,1) Padé transformation with respect to δ as done by Duncan and Moshe [3] (the (0,2) transformation gives no extrema at all). One finds a relevant minimum for all β above $\beta_{pi} = 1.0486$. The results are again presented in fig. 2a. They show considerable improvement compared to the first order and already a very close agreement with the MC data.

Order 3

In order three there are 16 types of connected configurations, 7 of them are lower order configurations with multiply occupied plaquettes. The correct counting of the number of equivalent members of one type becomes delicate for some cases but is still feasible. We refer to fig. 1c for details.

There is now again a reasonable weak coupling limit. For large β there is an extremum at $\lambda \approx 0.2234/\beta$ for $d = 4$ which leads to $E \approx 1 - 0.2417/\beta$. The error in the coefficient of $1/\beta$ has become smaller by a factor of 3.4 compared to the first order. If one decreases β and follows the minimum, the latter disappears at $\beta_{pi} = 1.2187$. But at some larger λ there is another minimum. One may switch to this with practically no change in the plaquette energy, and go further down to $\beta_{pi} = 1.0625$ where this minimum also disappears. The result shows only a minor change compared to the second order and there is thus again excellent agreement with the data.

As in the first order one can now again enlarge the region of applicability by the power trick or the Padé transformation. Only the (0,3) transformation works, the (2,1) and the (1,2) transformation show no extrema below the transition region. The results are shown in fig. 2b. Again the power curve lies below the Padé curve and both of

them are much closer to the data below the phase transition than in first order. The discrepancy is, however still sizeable in this region. For $\beta > 1.1$ both curves practically agree with the ordinary third order curve.

Order 4

The simplicity of our approach permits to go up to fourth order with reasonable effort for $d = 3$ and $d = 4$. To do this we wrote a computer program in Mathematica. It searches all possibilities for connected plaquettes in a certain order. Some configurations which are obtained from others by permutations of p_1, \dots, p_n are not found in this way, while others which involve multiply occupied plaquettes are obtained several times. This is taken into account by applying the appropriate factors. Finally the program calculates the contribution for each configuration and adds up everything. This program also served as a check for the lower order calculations.

As in the second order we apply a Padé transformation. The only useful one turned out to be the (2,2) diagonal transformation. There are two intervals in β where the use of the relevant extrema gives good, respectively excellent, agreement with the data, as seen in fig. 2a. The first one is *below* the transition region and impressively reproduces the steep increase of the plaquette energy in this region. For $\beta > 1.08$, however, the curve lies above the data. There is a second interval, $1.4 < \beta < \infty$, where one has perfect agreement with the data. For $\beta < 1.4$, however, the curve lies again too high.

Other dimensions

The discussion proceeds as before, therefore we can be very brief here. In first order the points where the minima disappear are at $\beta_{pi} = 1.1937$ for $d = 3$ and at $\beta_{pi} = 0.8099$ for $d = 5$. The results are shown in figs. 3a and 4a, the curves obtained with the power trick and the (0,1) Padé transformation in figs. 3b and 4b. In second order the limiting values for the (1,1) Padé transformations are $\beta_{pi} = 1.4495$ for $d = 3$ and $\beta_{pi} = 0.8090$ for $d = 5$. In third order one finds the following common feature for large β : For increasing λ there are two minima and two maxima at finite λ , the extremum at lowest λ is the relevant minimum. If one decreases β , there is a qualitative difference for different dimensions. In the case $d = 3$, the first minimum and maximum merge into a point of inflexion at some β_{pi} . The second pair merges already for slightly larger β , but this is of no importance, because these extrema are not relevant. For $d = 4$ and $d = 5$, on the other hand, the first pair merges at a larger β than the second one, so one has to jump to the second minimum for a short interval till this also disappears. For $d \geq 6$, finally, the irrelevant interior pair of extrema merges first, for still smaller β the outer pair merges into a point of inflexion. This means that for $d = 3$, as well as for $d \geq 6$, one can follow the minimum down to the critical value, while for $d = 4$ and $d = 5$ one has to jump to the other minimum near the phase transition. Clearly the results are much better in five dimensions than in three. This is due to the above mentioned error in the coefficient of the weak coupling expansion which becomes smaller for larger dimension.

4 SU(2)

We use the notation of Creutz [11], Lautrup and Nauenberg [12], and Buckley and Jones [5], with $(\beta/2) \sum_{p'} \text{Tr} U_{p'}$ in the exponent, and the plaquette energy defined as the expectation value of $(1/2) \text{Tr} U_p$. In the non abelian case it becomes crucial to choose an appropriate parametrization for the unitary matrices U_l on the links. A very convenient parametrization with a simple behavior in the weak coupling limit is the one proposed by Buckley and Jones [5]

$$U = e^{i\sigma_1\varphi} e^{i\sigma_2\vartheta} e^{i\sigma_3\psi}. \quad (4.1)$$

As parameter space one may use the region

$$-\pi < \varphi, \psi < \pi, \quad -\pi/4 < \vartheta < \pi/4. \quad (4.2)$$

Actually the group manifold is covered twice by this choice, but in this way we will already get periodicity in φ and ψ immediately. The Haar measure, in a normalization convenient for us, reads

$$H(\psi, \vartheta, \varphi) = \frac{\pi}{2} \cos(2\vartheta). \quad (4.3)$$

An efficient technique for the further procedure, which was also extensively used in [5], is the splitting of the matrix exponentials in (4.1) into sums of ordinary exponentials times projection operators, in general

$$e^{i\sigma_k\alpha} = \sum_{s=\pm 1} e^{is\alpha} P_s^{(k)}, \quad \text{with} \quad P_s^{(k)} = \frac{1}{2}(1 + s\sigma_k). \quad (4.4)$$

From this it is immediately clear that all traces are periodic functions of the three link angles $\varphi_l, \vartheta_l, \psi_l$ with period 2π . So, for φ and ψ we may use the same procedure as in the U(1) case, in order to extend the integrations from $-\infty$ to ∞ . For the ϑ integration, on the other hand, the presence of the Haar measure and the limited integration region from $-\pi/4$ to $\pi/4$ enforce a special procedure. We have to continue the Haar measure periodically into the full interval from $-\pi$ to π by expanding it into a Fourier series. This results in

$$\frac{\pi}{2} \cos(2\vartheta)_{\text{periodic}} = \sum_{\nu=-\infty}^{\infty} \frac{(-1)^\nu e^{4i\nu\vartheta}}{1 - 4\nu^2}. \quad (4.5)$$

The unitary matrices U in (4.1) can be decomposed into a linear combination of $1, \sigma_k$. It is then easily seen that they are invariant under the substitution $\vartheta \rightarrow \pi/2 - \vartheta$, if, simultaneously, one substitutes $\varphi \rightarrow \varphi + \pi/2, \psi \rightarrow \psi + \pi/2$. The integral is invariant under the latter substitutions due to the periodicity in φ and ψ . Together with similar relations, the ϑ -integration can thus also be extended to the interval from $-\pi$ to π and subsequently from $-\infty$ to ∞ if we use the periodic Haar measure in (4.5).

Next we introduce again the continuum fields $A_\mu^{(a)}$, the longitudinal components on the links are connected to the link angles by

$$\varphi = \frac{g}{2} \int \mathbf{A}^{(1)} d\mathbf{x}, \quad \vartheta = \frac{g}{2} \int \mathbf{A}^{(2)} d\mathbf{x}, \quad \psi = \frac{g}{2} \int \mathbf{A}^{(3)} d\mathbf{x}, \quad \text{with } g^2 = 4/\beta. \quad (4.6)$$

Contrary to the abelian $U(1)$ case the procedure is now no longer gauge invariant, because we introduce an ordinary exponential, not a path ordered exponential, along the link. We have, of course, the freedom to do this.

Next we introduce the free interpolating action as in (2.7), with the sole difference that we have to sum over the three $SU(2)$ indices a in the potentials $A_\mu^{(a)}$. The situation is now quite similar to the abelian case. The expansion for $E^{(n)}$ looks as in (2.15), (2.16) where now $E_p = (1/2)\text{Tr}U_p$. Again only connected configurations of plaquettes contribute in the expansion.

The plaquette actions, when evaluated by using (4.4), contain 10 (not 12) projection operators, because two of the unitary matrices enter as adjoints, and neighboring identical σ - matrices can be combined. The traces are therefore 10 fold sums with 2^{10} terms. The plaquette angles appear in exponentials only. The path integrations over φ and ψ (more precisely, those over $A_\mu^{(1)}$ and $A_\mu^{(3)}$) can be performed as before. In the ϑ - integrations one has to consider in addition the periodic continuation of the Haar measure (4.5), which also only contains exponentials. In this way the following functions, defined by infinite sums, arise:

$$f_m(\lambda) = \sum_{\nu=-\infty}^{\infty} \frac{(-1)^\nu e^{-(4\nu+m)^2 \lambda/4}}{1 - 4\nu^2} \quad (4.7. a)$$

$$h_m(\lambda) = f_m(\lambda)/f_0(\lambda). \quad (4.7. b)$$

Up to second order we will only need the functions $h_m(\lambda)$ for $m = 1, 2, 3$, obviously $h_m(\lambda) = h_{-m}(\lambda)$. The sums in (4.7) converge rapidly, therefore the consideration of a few terms is sufficient for the computation.

The evaluation of the full traces is only necessary in the case of multiply occupied plaquettes. In all configurations where links belong to one plaquette only, it is much simpler to perform the integrations over the corresponding link variables first. This removes the corresponding σ - matrices and leads to much simpler traces. For m -fold occupied plaquettes, on the other hand, a calculation by brute force becomes prohibitively complicated very soon, because it would involve a sum over 2^{10m} terms! Fortunately one can reduce the complexity of the problem by using a simple group theoretical relation:

$$[\text{Tr}U_{1/2}]^2 = 1 + \text{Tr}U_1. \quad (4.8)$$

Here $U_{1/2}$ and U_1 denote the $SU(2)$ representation matrices in the spin 1/2 and 1 representation respectively. The latter are simply related to the former by replacing $e^{i\sigma_k \alpha}$ by $e^{i2J_k \alpha}$, with J_k the 3×3 representation matrices. Application of (4.8) reduces the complexity, but not quite as much as it appears at first sight. The matrices J_k fulfil $J_k^{2n} = J_k^2$ for $n \geq 1$ and $J_k^{2n+1} = J_k$ for $n \geq 0$. Contrary to the spin 1/2 case, however, $J_k^2 \neq 1$. Therefore the relation corresponding to (4.4) is slightly more complicated:

$$e^{i2J_k\alpha} = \sum_{s=0,\pm 1} e^{i2s\alpha} \bar{P}_s^{(k)}, \quad \text{with} \quad \bar{P}_0^{(k)} = 1 - J_k^2, \quad \bar{P}_{\pm 1}^{(k)} = \frac{1}{2}(J_k^2 \pm J_k). \quad (4.9)$$

Nevertheless, the simplification obtained by using (4.8) is sizeable. E.g. for the twofold occupied plaquette it reduces the number of terms in the sum from 2^{20} to 3^{10} , i.e. by a factor of ≈ 18 . In this way it was possible to calculate all contributions of the second order without special effort, except the threefold plaquette. But fortunately the latter appears only once and can be safely neglected among the 977 configurations which contribute in second order.

After these remarks we can come to the results:

Order 1

The first order result reads

$$\begin{aligned} E^{(1)}(\beta, \lambda) = & \\ & [1 + \delta\lambda(-2 + 4h_1'(\lambda)/h_1(\lambda))e^{-2\lambda}h_1^4(\lambda) \\ & + \delta\beta[(1 + e^{-8\lambda} + 2e^{-4\lambda}h_2^4(\lambda))/4 - e^{-4\lambda}h_1^8(\lambda)] \\ & + \delta\beta(2d - 3)\left[\frac{1}{2}e^{-3\lambda}h_1^6(\lambda)\{(1 + e^{-\lambda})^2(1 + h_2(\lambda)) + (1 - e^{-\lambda})^2(1 - h_2(\lambda))\}\right. \\ & \left. - 4e^{-4\lambda}h_1^8(\lambda)\right]. \end{aligned} \quad (4.10)$$

The first term with $\delta\beta$ arises from the double plaquette, the second one from the neighboring plaquettes. The whole situation is rather similar to the U(1) case. The minimum with respect to λ now disappears at $\beta_{pi} = 2.1377$. In fig. 5 we show the result, together with the one obtained by the power trick and the (0,1) Padé transformation. The quality of the results is comparable to the U(1) case.

Order 2

The extremum disappears at $\beta_{pi} = 2.2336$, the corresponding energy lies somewhat above the data. For increasing β , however, the curve drops down below the data as in the U(1) case which shows again the problematics of even orders of the expansion. We therefore performed the (1,1) Padé transformation as before. It has an extremum for all β above $\beta_{pi} = 2.2737$. The result is also shown in fig. 5. The second order Padé transformation reduces the error by a factor of about one half compared to the first order. The agreement with the data is not as good as for U(1) in $d = 4$. The poorer quality of the approximation in the non abelian case could be due to the specific gauge dependence introduced by our definition of the fields in (4.6), or to the non analyticity in ϑ resulting from the periodic continuation of the Haar measure in (4.5).

5 Conclusions

The present work can be considered as an empirical study of the convergence properties of the optimized δ - expansion for non trivial systems with an infinite number of degrees of freedom and possibly a phase transition. Because we were able to go up to fourth order in the case of U(1) in $d = 4$ dimensions, we believe that our conclusions can be considered as quite reliable. We begin with the positive aspects:

For β above the critical value β_c of the phase transition, one has rapid convergence in the whole region. The second order (1,1) Padé transformation gives already perfect agreement with the MC data.

For $\beta < \beta_c$ one needs manipulations like the power trick or a suitable Padé transformation in order that the principle of minimal sensitivity can be applied down to lower β . The discrepancy with the data is much larger in this region, but a clear tendency of convergence towards the latter is visible. The fourth order (2,2) Padé transformation gives a remarkably good approximation down to $\beta > 0.95$ which hardly can be considered as accidental. The large increase of the energy within a small region of β is clearly reproduced. This result exceeds the previous work in refs [3] -[7] where good approximations were obtained up to the transition region (from above or from below, respectively) but not beyond. Unfortunately higher order calculations appear not feasible with reasonable effort without an additional idea. In the case of U(1) it is quite trivial to write down the contribution for any configuration with the help of (2.19); the only cumbersome task is the correct counting of equivalent configurations. Rigorous convergence proofs for complex systems as considered here are also not available. So one can only speculate that higher orders would stay stable above the transition region and further improve the results below.

Let us finally mention the dubious aspects of the whole approach. Its “distinctly alchemical flavor” [9] has clearly shown up again. The ambiguity in the choice of the interpolating action appears only as a minor deficiency; this choice is an art as in all variation methods. A really serious problem is that we have no a priori principle whatever, which tells us which of several extrema should be chosen. Even worse, there are cases, as in the even orders, where extrema exist in some β -interval, but none of them belongs to the physical situation. There are two possibilities how to find the relevant extremum, or, alternatively, to reject them all. The first one is to use additional, at least crude, information, say from MC data. The second one, which relies completely on the expansion itself, is to look for the convergence of the solution by comparing different orders of the expansion. Both criteria can be successfully applied to our figures. In view of the described general problematics it appears even more impressive, how the choice of the “correct” extremum leads to excellent results. This should encourage further theoretical work on the method.

References

- [1] P. M. Stevenson, Phys. Rev. D 23 (1981) 2916
- [2] D. Gromes, hep-9509224, Z. Phys. C (1996) in press
- [3] A. Duncan, M. Moshe, Phys. Lett. B 215 (1988) 352
- [4] A. Duncan, H. F. Jones, Nucl. Phys. B 320 (1989) 189
- [5] I. R. C. Buckley, H. F. Jones, Phys. Rev. D 45 (1992) 654
- [6] I. R. C. Buckley, H. F. Jones, Phys. Rev. D 45 (1992) 2073
- [7] J. O. Akeyo, H. F. Jones, Phys. Rev. D 47 (1993) 1668; Z. Phys. C 58 (1993) 629
- [8] D. G. Caldi, Nucl. Phys. B 220[FS8] (1983) 48
- [9] I. R. C. Buckley, A. Duncan, H. F. Jones, Phys. Rev. D 47, (1993) 2554;
A. Duncan, H. F. Jones, Phys. Rev. D 47 (1993) 2560
- [10] G. Bhanot, M. Creutz, Phys. Rev. D 21 (1980) 2892
- [11] M. Creutz, Phys. Rev. D 21 (1980) 2308
- [12] B. Lautrup, M. Nauenberg, Phys. Rev. Lett. 45 (1980) 1755

Figure Captions

Fig. 1a,b,c: The connected plaquette configurations for order 1, 2, and 3

Together with each generic type we give the number of configurations of this type for arbitrary dimension d . In order 3 the types 8 and 9 give identical contributions, the same holds for type 10 and 11. One has to note, that, e.g. the symbol for type 8 in fig. 1c stands for all types of configurations with the same topology. As an example, some of them are shown in fig. 1d.

Fig. 1d: Some examples for configurations belonging to type 8 of fig. 1c

Fig. 2a: The U(1) plaquette energy in 4 dimensions near and above the transition region

Upper dashed line (long dashes): First order

Dashed line (normal dashes): Second order diagonal Padé transformation

Dashed line (short dashes): Third order

Solid lines: Fourth order diagonal Padé transformation

The MC data are taken from [8], where also references to earlier work can be found.

Fig. 2b: The U(1) plaquette energy in 4 dimensions extended below the transition region

Upper dashed line: First order (0,1) Padé transformation

Lower dashed line: First order power transformation with the limiting exponent $\kappa_0 = 0.2781$, for which the continuation to small β becomes possible

Upper solid line: Third order (0,3) Padé transformation

Lower solid line: Third order power transformation with limiting exponent $\kappa_0 = 0.4182$

The MC data are again taken from [8].

Fig. 3a: The U(1) plaquette energy in 3 dimensions near and above the transition region

Upper dashed line (long dashes): First order

Dashed line (normal dashes): Second order diagonal Padé transformation

Dashed line (short dashes): Third order

Solid lines: Fourth order diagonal Padé transformation

The MC data are taken from [10].

Fig. 3b: The U(1) plaquette energy in 3 dimensions extended below the transition region.

Upper dashed line: First order (0,1) Padé transformation
Lower dashed line: First order power transformation with limiting exponent $\kappa_0 = 0.5567$
Upper solid line: Third order (0,3) Padé transformation
Lower solid line: Third order power transformation with limiting exponent $\kappa_0 = 0.5497$
The MC data are again taken from [10].

Fig. 4a: The U(1) plaquette energy in 5 dimensions near and above the transition region

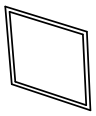
Upper dashed line (long dashes): First order
Dashed line (normal dashes): Second order diagonal Padé transformation
Solid line: Third order
The MC data are taken from [10].

Fig. 4b: The U(1) plaquette energy in 5 dimensions extended below the transition region.

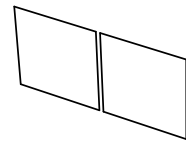
Upper dashed line: First order (0,1) Padé transformation.
Lower dashed line: First order power transformation with limiting exponent $\kappa_0 = 0.0410$
Upper solid line: Third order (0,3) Padé transformation
Lower solid line: Third order power transformation with limiting exponent $\kappa_0 \approx 0$
The MC data are again taken from [10].

Fig. 5: The SU(2) plaquette energy in 4 dimensions.

Dashed line ending at cross (short dashes): First order
Dashed line (normal dashes): First order (0,1) Padé transformation
Dashed line (long dashes): First order power transformation with limiting exponent $\kappa_0 = 0.3968$
Solid line: Second order (1,1) Padé transformation
The MC data are from [12].

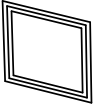


$$N_1=1$$

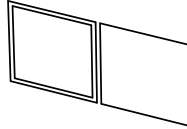


$$N_2=4(2d-3)$$

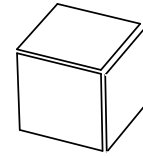
Fig. 1a: The connected plaquette configurations for order 1



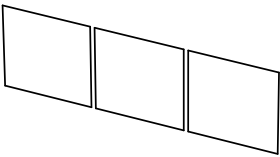
$$N_1=1$$



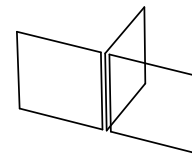
$$N_2=12(2d-3)$$



$$N_3=8(2d-4)$$



$$N_4=12(12d^2-40d+35)$$



$$N_5=4(2d-3)(2d-4)$$

Fig. 1b: The connected plaquette configurations for order 2

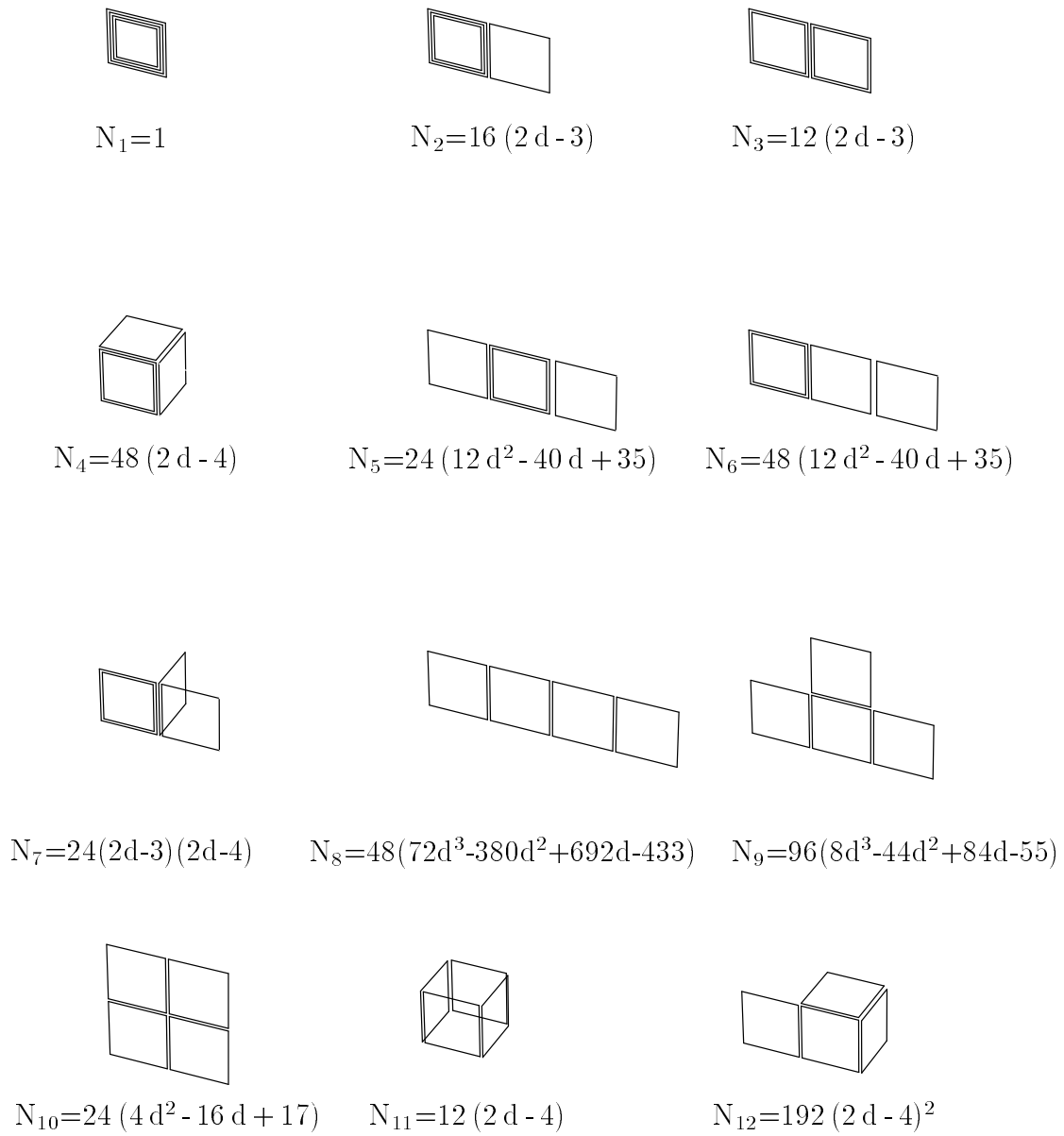
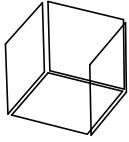
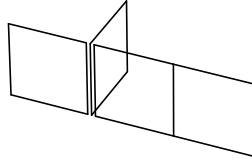


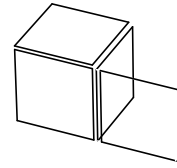
Fig. 1c: The connected plaquette configurations for order 3



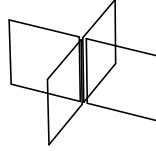
$$N_{13}=48(2d-4)$$



$$N_{14}=48(2d-4)(12d^2-44d+43)$$



$$N_{15}=96(2d-4)^2$$



$$N_{16}=4(2d-3)(2d-4)(2d-5)$$

Fig. 1c (cont.): The connected plaquette configurations for order 3

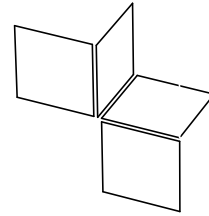
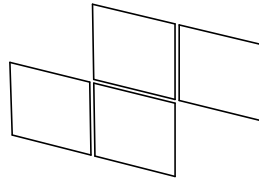
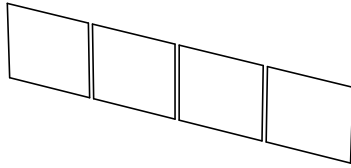


Fig. 1d: Some examples for configurations belonging to type 8 of fig. 1c

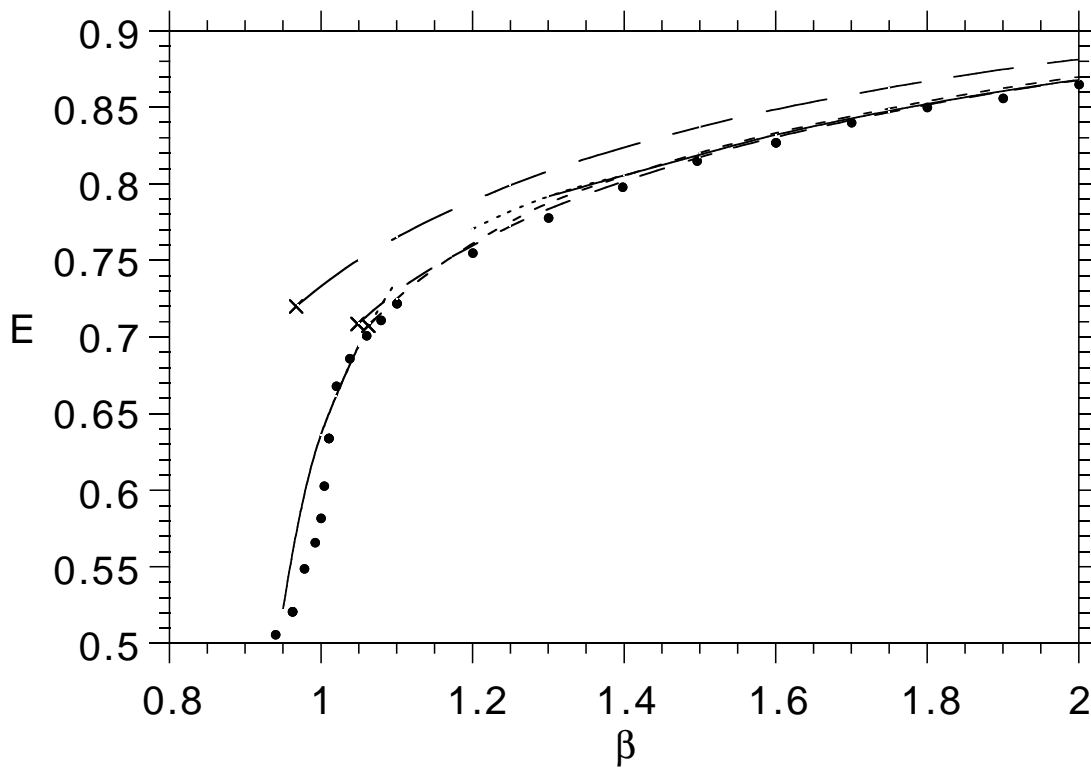


Fig. 2a: The U(1) plaquette energy in 4 dimensions near and above the transition region

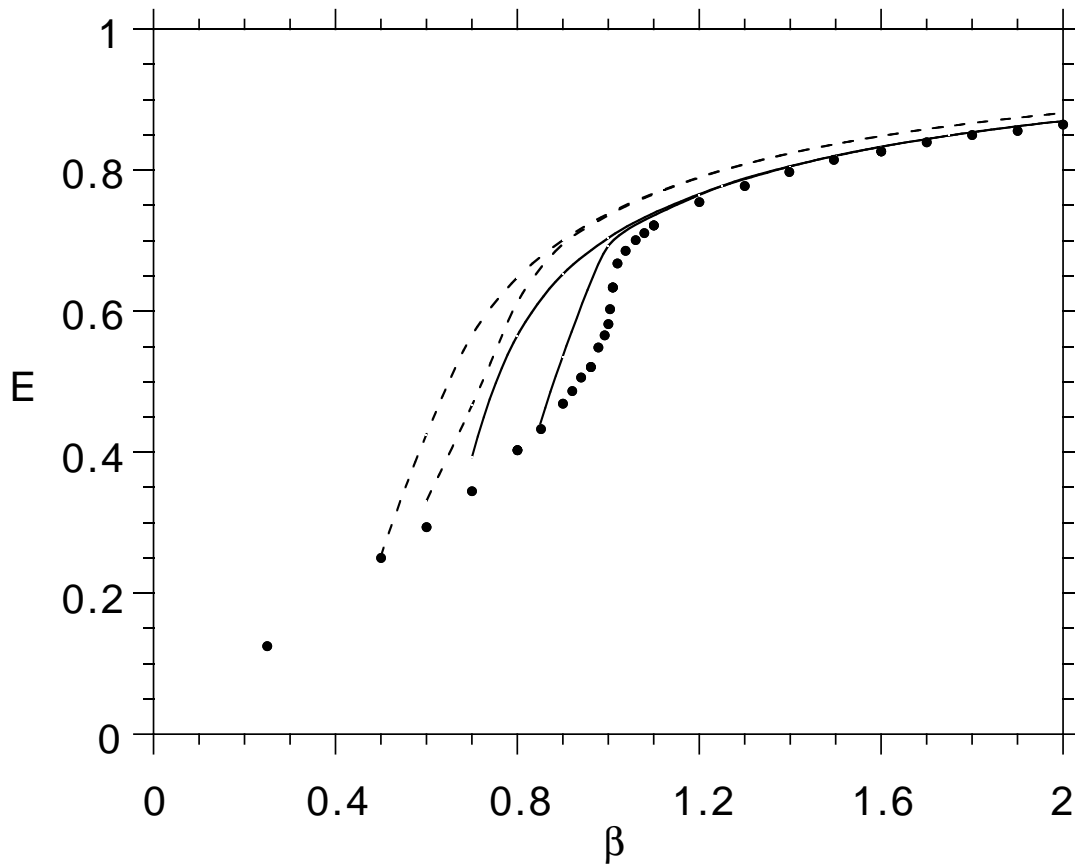


Fig. 2b: The U(1) plaquette energy in 4 dimensions extended below the transition region

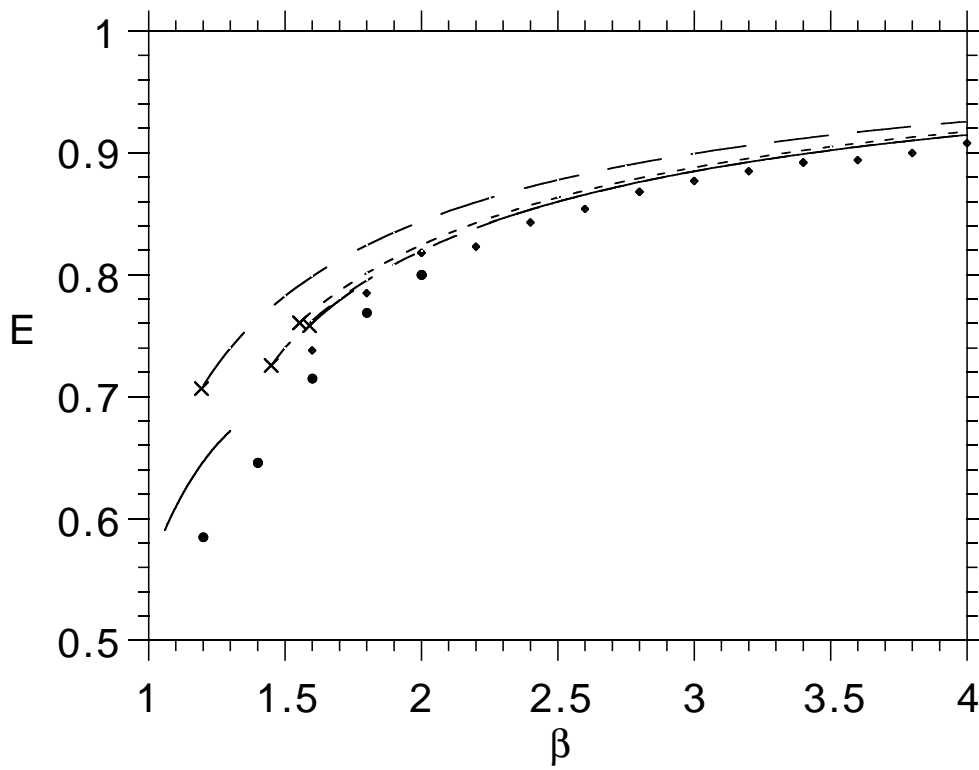


Fig. 3a: The U(1) plaquette energy in 3 dimensions near and above the transition region

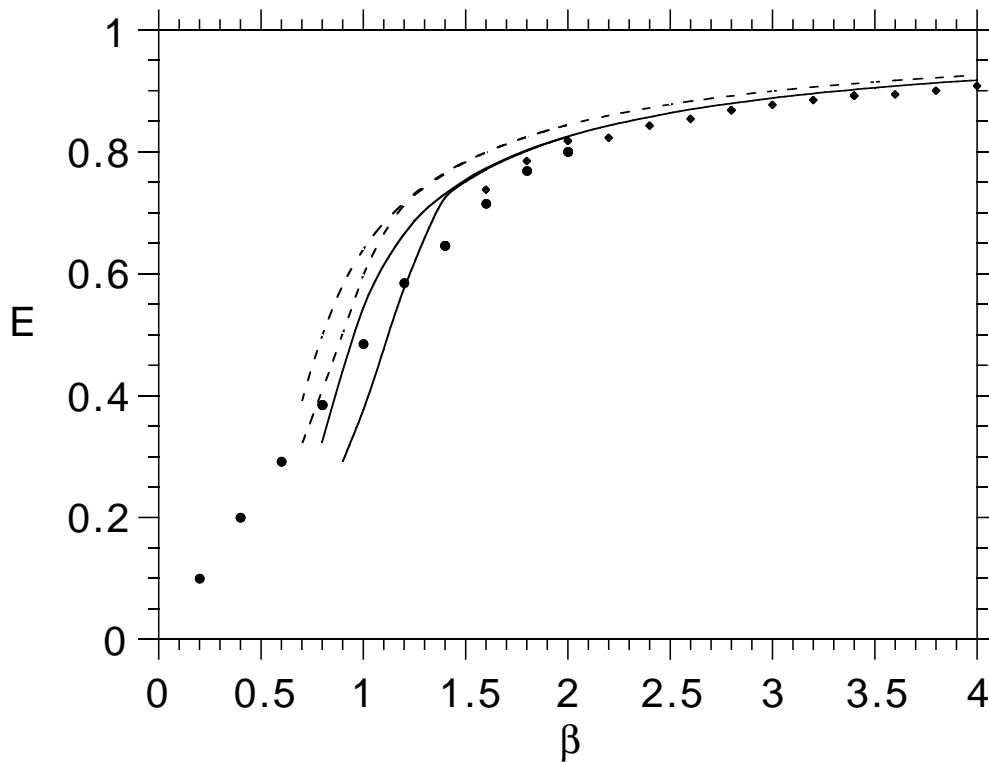


Fig. 3b: The U(1) plaquette energy in 3 dimensions extended below the transition region

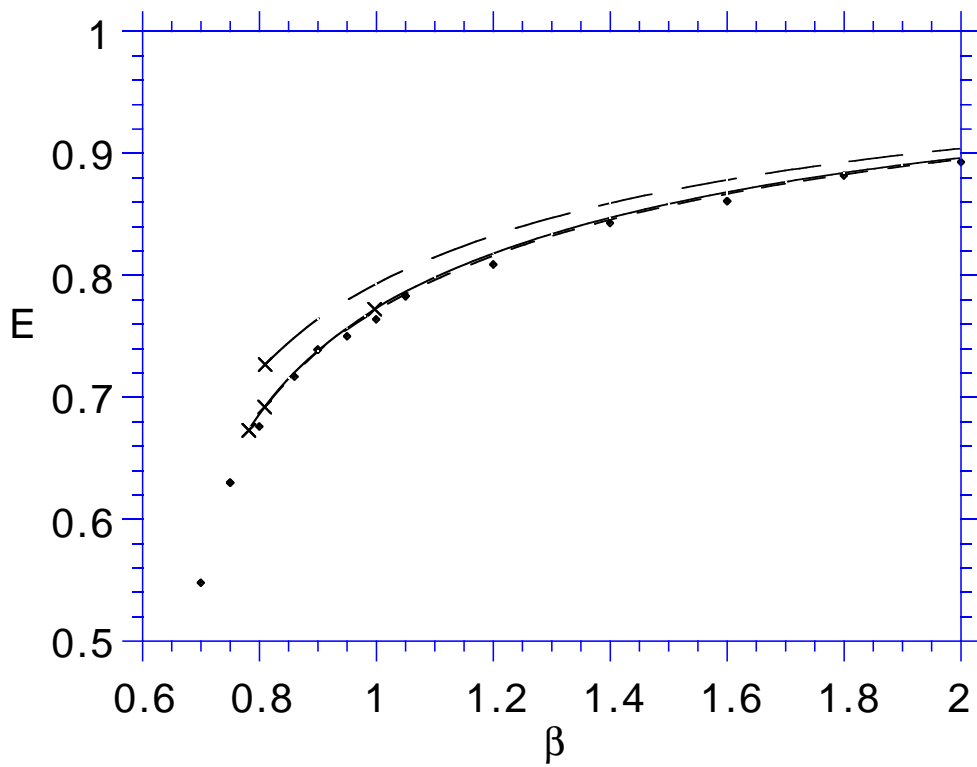


Fig. 4a: The U(1) plaquette energy in 5 dimensions near and above the transition region

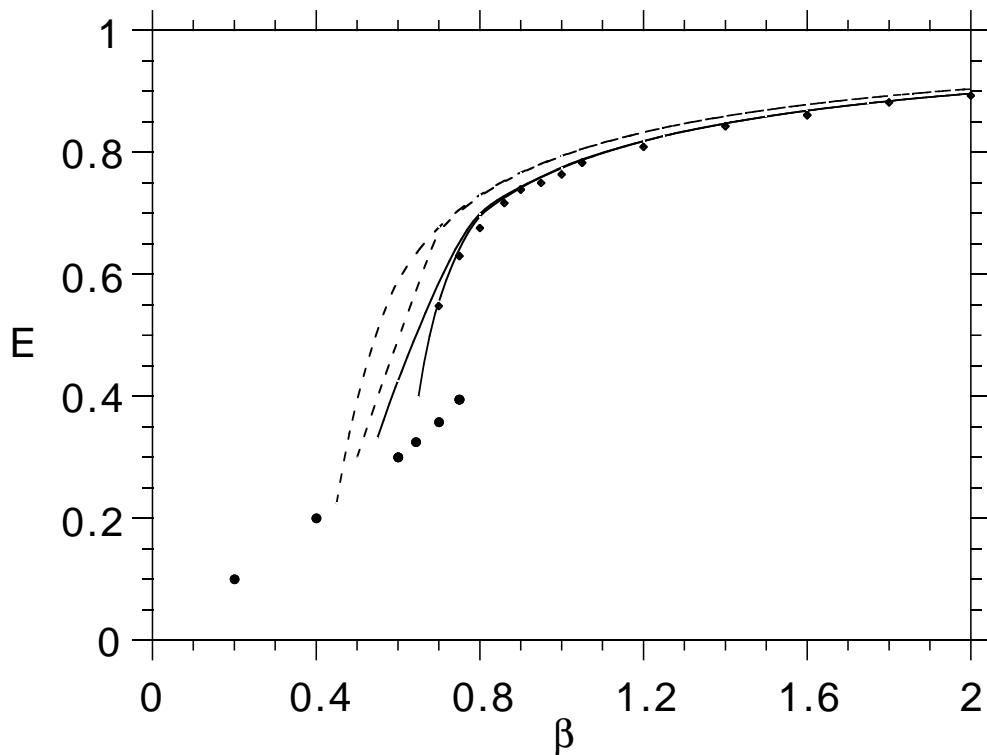


Fig. 4b: The U(1) plaquette energy in 5 dimensions extended below the transition region

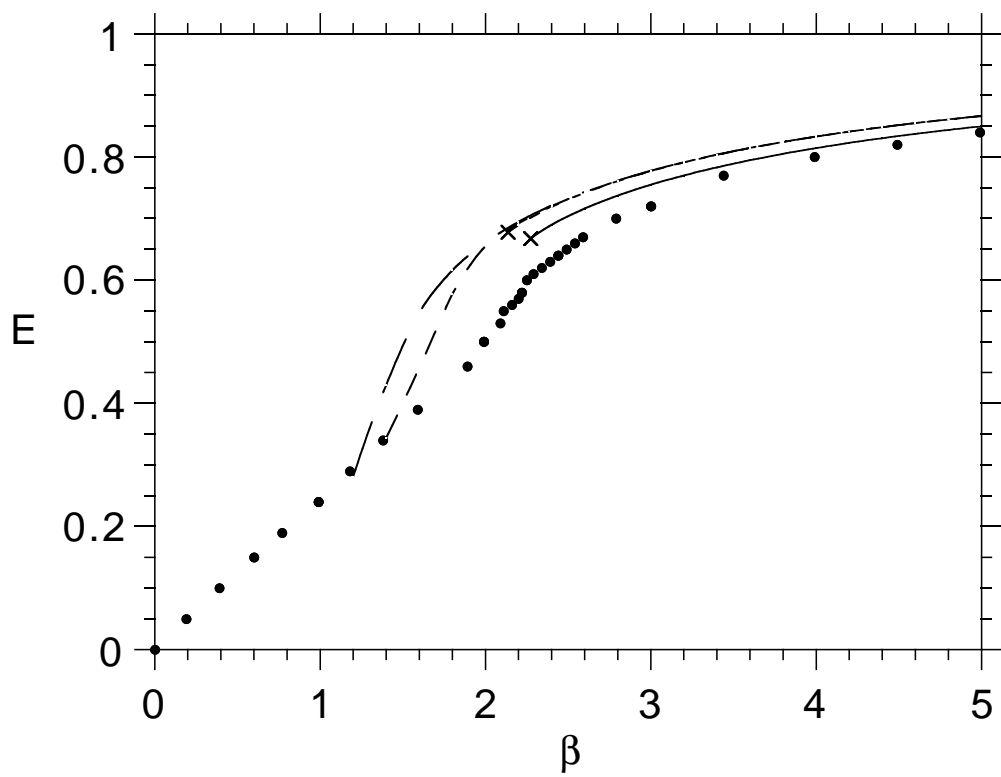


Fig. 5: The SU(2) plaquette energy in 4 dimensions